Inorg. Chem. **2007**, *46*, 1305−1314

Intramolecular Chalcogen−Tin Interactions in (o-MeE-C_6H_4)$CH_2SnPh_{3-n}Cl_n$ (E = S, O; n = 0, 1, 2), Characterized by X-ray Diffraction and ^{119}Sn Solution and Solid-State NMR

Teresita Munguia, Marcela López-Cardoso,† Francisco Cervantes-Lee, and Keith H. Pannell*

Department of Chemistry, University of Texas at El Paso, El Paso, Texas 79968-0513

Received September 22, 2006

Organotin(IV) compounds of the type (o-MeE-C_6H_4)$CH_2SnPh_{3-n}Cl_n$ were synthesized, E = O, n = 0 (**1**), n = 1 (**2**), n = 2 (**3**) and E = S, n = 0 (**4**), n = 1 (**5**), n = 2 (**6**). The complexes exhibit significant trigonal bipyramidal pentacoordination at tin as a consequence of intramolecular Sn–O (**1**–**3**) and Sn–S (**4**–**6**) interactions upon substitution of the phenyl groups by chloro groups. The intramolecular Sn–O distances in **1**, **2**, and **3** are 83%, 75%, and 79% of the sum of the van der Waals radii. The equivalent Sn–S values for **4**, **5**, and **6** are 90%, 73%, and 71%, respectively. The geometry of compound **3** is complicated by intermolecular dimerization via bridging chlorines creating a distorted octahedral geometry at tin. The related dichloro sulfur compound **6** also exhibits an intermolecular association in the form of Sn–Cl–H hydrogen bonding leading to a polymeric structure in the solid state. CPMAS ^{119}Sn NMR spectroscopy suggests that the intramolecular Sn–E interactions persist in solution and also facilitated the discovery of a new crystalline form of **4**, **4′**, that contains a Sn–S distance which is 95% the sum of the van der Waals radii.

Introduction

The ability of tetravalent tin to be coordinated effectively by Lewis bases such as N, S, and O, leading to penta- and hexa-coordinated structures, via both inter- and intramolecular interactions, is well-established.[1] Such intermolecular interactions are thought to contribute to the bioactivity of triorganotin compounds.[2] For example, two specific triethyltin binding sites were found in rat liver mitochondria, a high-affinity site involving histidine residues and a low-affinity site associated with thiol groups.[3] Nath[4,5] and others[2,6] have shown that the bioactive organotin species is $R_nSn^{(4-n)+}$ (n = 2, 3). Given this understanding, the design of organotins with potential intramolecular coordination to S and O is of interest to us as a means of seriously modifying the bioavailability of the active tin species, Figure 1.[7]

Compounds in which tin has the capacity to intramolecularly interact with sulfur or oxygen are well-studied, and several reviews of the subject can be found.[7,8] There are two major groups of organotins with such E−Sn intramolecular interactions: (A) the 1,1-dithiolates or η^2-(O,O′)-carboxylates, Figure 2a,[9,10] and (B) systems that bring oxygen or sulfur close to tin via "arms" of various carbon length as

* To whom correspondence should be addressed. E-mail: kpannell@utep.edu.

† Present address: Centro de Investigaciones Químicas, Universidad Autónoma de Estado de Morelos, Avenida Universidad 1001, Chamilpa, Cuernavaca, 62210 Morelos, México.

(1) (a) Davies, A. G. In *Comprehensive Organometallic Chemistry II*; Abel, E. W.; Stone, F. G. A.; Wilkinson, G., Eds.; Elsevier Science Inc.: Tarrytown, NY, 1995; Vol. 2. (b) Harrison, P. G. Compounds of Tin: General Trends. In *Chemistry of Tin*; Harrison, P. G., Ed.; Chapman and Hall: New York, 1989.

(2) Swisher, R. G.; Vollano, J. F.; Chandrasekhar, V.; Day, R. O.; Holmes, R. R. *Inorg. Chem.* **1984**, *23*, 3147−3152.

(3) (a) Rose, M. S.; Lock, E. A. *Biochem. J.* **1970**, *120*, 151 (b) Farrow, B. G.; Dawson, A. P. *Eur. J. Biochem.* **1978**, *86*, 85−95.

(4) (a) Nath, M.; Pokharia, S.; Eng, G.; Song, X.; Kumar, A. *J. Organomet. Chem.* **2003**, *669*, 109−123. (b) Nath, M.; Pokharia, S.; Eng, G.; Song, X.; Kumar, A.; Gielen, M.; Willem, R.; Biesemans, M. *Appl. Organomet. Chem.* **2004**, *18*, 460−470. (c) Nath, M.; Pokharia, S.; Song, X.; Eng, G.; Gielen, M.; Kemmer, M.; Biesemans, M.; Willem, R.; de Vos, D. *Appl. Organomet. Chem.* **2003**, *17*, 305−314. (d) Nath, M.; Pokharia, S.; Yadav, R. *Coord. Chem. Rev.* **2001**, *215*, 99−149.

(5) Nath, M.; Pokharia, S.; Eng, G.; Song, X.; Kumar, A. *Spectrochim. Acta, Part A* **2006**, *63A*, 66−75.

(6) Gajda-Schrantz, K.; Jancso, A.; Pettinari, C.; Gajda, T. *J. Chem. Soc., Dalton Trans.* **2003**, 2919−2916.

(7) Munguia, T.; Cervantes-Lee, F.; Párkányi, L. Organotin−Sulfur Intramolecular Interactions: An Overview of Current and Past Compounds and the Biological Implications of Sn−S Interactions. In *Modern Aspects of Main Group Chemistry*; Lattman, M., Kemp, R. A., Eds.; American Chemical Society: Washington, DC, 2006; Vol. 917, pp 422−435.

(8) (a) Tiekink, E. R. T. *Appl. Organomet. Chem.* **1991**, *5*, 1−23. (b) Tiekink, E. R. T. *Main Group Met. Chem.* **1992**, *15*, 161−186.

10.1021/ic061811s CCC: $37.00
Published on Web 01/24/2007

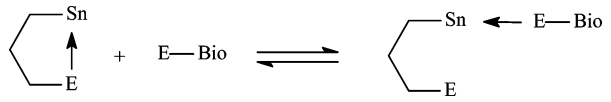

Figure 1. Potential competition for coordination between biological residues and ligands associated via intramolecular interactions.

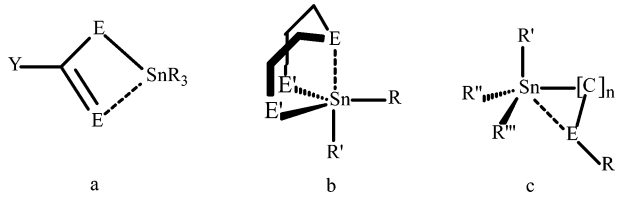

Figure 2. (a) General structure for 1,1-dithiolates and η^2-(*O*,*O*′)-carboxylates. E = O, S; Y = NR_2, OR, aryl/alkyl (b) Stannocanes which bring O or S in close proximity to Sn by 1,5 transannular interaction. E = O, S; E′= C, S (c) Compounds which bring O, S close to Sn via carbon chains of varying length. E can be an ether, carbonyl oxygen, or thioether.

studied by Dräger[11−13] and others,[14,15] Figure 2b,c. The oxygen at the end of the carbon chain can be an ether or a carboxyl moiety,[16,17] whereas the majority of the sulfur systems involve simple aryl or alkyl sulfides.[7,18−20]

Although our main focus is on tin chalcogen interactions, it is interesting to note that an analogous compound with an amino group in the ortho position has been reported.[21] The only crystal structure reported, however, is MePh[2-Me_2-$NC_6H_4CH(SiMe_3)$]SnBr in which the N−Sn distance is 2.492(3) Å (63% of the sum of the van der Waals radii for Sn and N). Analogous compounds with the tin moiety in the ortho position and the amino group on the benzyl carbon exhibit intramolecular N−Sn distances ranging from 2.47-(1) to 3.68(2) Å.[22]

The degree of intramolecular E−Sn bonding is usually assessed by single-crystal X-ray diffraction, Mössbauer spectroscopy,[5,23] and less extensively to date, solid-state ^{119}Sn NMR spectroscopy.[10,24−26] We now report the synthesis, single-crystal structural characterization, and ^{119}Sn CPMAS NMR of a group of previously unknown organotins of the

(9) (a) Lockhart, T. P.; Manders, W. F.; Schlemper, E. O. *J. Am. Chem. Soc.* **1985**, *107*, 7451−7453. (b) Tani, K.; Kato, S.; Kanda, T.; Inagaki, S. *Org. Lett.* **2001**, *3*, 655−657. (c) Tiekink, E. R. T.; Winter, G. *J. Organomet. Chem.* **1986**, *314*, 85−89. (d) Wengrovius, J. H.; Garbauskas, M. F. *Organometallics* **1992**, *11*, 1334−1342. (e) Hook, J. M.; Linahan, B. M.; Taylor, R. L.; Tiekink, E. R. T.; van Gorkom, L.; Webster, L. K. *Main Group Met. Chem.* **1994**, *17*, 293−311. (f) Holt, E. M.; Nasser, F. A. K.; Wilson, A.; Zuckerman, J. J. *Organometallics* **1985**, *4*, 2073−2080. (g) Hall, V. J.; Tiekink, E. R. T. *Main Group Met. Chem.* **1995**, *18*, 611−620. (h) Donoghue, N.; Tiekink, E. R. T. *J. Organomet. Chem.* **1991**, *420*, 179−184. (i) Das, V. G. K.; Wei, C.; Sinn, E. *J. Organomet. Chem.* **1985**, *290*, 291−299. (j) Kana, A. T.; Hibbert, T. G.; Mahon, M. F.; Molloy, K. C.; Parkin, I. P.; Price, L. S. *Polyhedron* **2001**, *20*, 2989−2995. (k) Kato, S.; Tani, K.; Kitaoka, N.; Yamada, K.; Mifune, H. *J. Organomet. Chem.* **2000**, *611*, 190−199. (l) Mohamed-Ibrahim, M. I.; Chee, S. S.; Buntine, M. A.; Cox, M. J.; Tiekink, E. R. T. *Organometallics* **2000**, *19*, 5410−5415. (m) Sheldrick, G. M.; Sheldrick, W. S. *J. Chem. Soc., (A)* **1970**, 490−493. (n) Sheldrick, G. M.; Sheldrick, W. S.; Dalton, R. F.; Jones, K. *J. Chem. Soc., A* **1970**, 493−497. (o) Tarassoli, A.; Sedaghat, T.; Neumuller, B.; Ghassemzadeh, M. *Inorg. Chim. Acta* **2001**, *318*, 15−22. (p) Vrabel, V.; Kello, E. *Acta Crystallogr.* **1993**, *C49*, 873−875. (q) Baul, T. S. B.; Rynjah, W.; Willem, R.; Biesemans, M.; Verbruggen, I.; Holèapek, M.; de Vos, D.; Linden, A. *J. Organomet. Chem.* **2004**, *689*, 4691−4701. (r) Khoo, L. E.; Goh, N. K.; Koh, L. L.; Xu, Y.; Whalen, D. J.; Eng, G. *Appl. Organomet. Chem.* **1996**, *10*, 459−465. (s) James, B. D.; Kivlighon, L. M.; Skelton, B. W.; White, A. H. *Appl. Organomet. Chem.* **1998**, *12*, 13−23. (t) Willem, R.; Bouhdid, A.; Mahieu, B.; Ghys, L.; Biesemans, M.; Tiekink, E. R. T.; de Vos, D.; Gielen, M. *J. Organomet. Chem.* **1997**, *531*, 151−158. (u) Imatiaz-un-Din; Mazhar, M.; Dastgir, S.; Mahon, M. F.; Molloy, K. C. *Appl. Organomet. Chem.* **2003**, *17*, 801−802. (v) Rénamy, S. V.; Bassène, S.; Diop, C. A. K.; Sidibé, M.; Diop, L.; Mahon, M. F.; Molloy, K. C. *Appl. Organomet. Chem.* **2004**, *18*, 455−459.

(10) Di Nicola, C.; Galindo, A.; Hanna, J. V.; Marchetti, F.; Pettinari, C.; Pettinari, R.; Eleonora, R.; Skelton, B. W.; White, A. H. *Inorg. Chem.* **2005**, *44*, 3094−3102.

(11) (a) Dräger, M.; Engler, R. *Chem. Ber.* **1975**, *108*, 17−25. (b) Dräger, M.; Engler, R. *Z. Anorg. Allg. Chem.* **1975**, *413*, 229−238. (c) Beuter, M.; Kolb, U.; Zickgraf, A.; Bräu, E.; Bletz, M.; Dräger, M. *Polyhedron* **1997**, *16*, 4005−4015.

(12) (a) Dräger, M.; Guttmann, H. J. *J. Organomet. Chem.* **1981**, *212*, 171−182. (b) Kolb, U.; Beuter, M.; Drager, M. *Organometallics* **1994**, *13*, 4413−4425.

(13) Kolb, U.; Beuter, M.; Drager, M. *Inorg. Chem.* **1994**, *33*, 4522−4530.

(14) (a) Cea-Olivares, R.; Lomeli, V.; Hernandez-Ortega, S.; Haiduc, I. *Polyhedron* **1995**, *14*, 747−755. (b) Garcia y Garcia, P.; Cruz-Almanza, R.; Toscano, R.-A.; Cea-Olivares, R. *J. Organomet. Chem.* **2000**, *598*, 160−166.

(15) Jurkschat, K.; Schilling, J.; Mugge, C.; Tzschach, A. *Organometallics* **1988**, *7*, 38−46.

(16) (a) Cea-Olivares, R.; Gómez-Ortiz, A.; García-Montalvo, V.; Gaviño-Ramírez, R.; Hernández-Ortega, S. *Inorg. Chem.* **2000**, *39*, 2284−2288. (b) Dakternieks, D.; Jurkschat, K.; Tozer, R.; Hook, J.; Tiekink, E. R. T. *Organometallics* **1997**, *16*, 3696−3706. (c) Deacon, P. R.; Devylder, N.; Hill, M. S.; Mahon, M. F.; Molloy, K. C.; Price, G. J. *J. Organomet. Chem.* **2003**, *687*, 46−56. (d) Jambor, R.; Dostal, L.; Ruzicka, A.; Cisarova, I.; Brus, J.; Holcapek, M.; Holecek, J. *Organometallics* **2002**, *21*, 3996−4004. (e) Jaumier, P.; Jousseaume, B. *Organometallics* **1997**, *16*, 5124−5126. (f) Kitagawa, O.; Fujiwara, H.; Suzuki, T.; Taguchi, T.; Shiro, M. *J. Org. Chem.* **2000**, *65*, 6819−6825. (g) Lébl, T.; Zoufalá, P.; Bruhn, C. *Eur. J. Inorg. Chem.* **2005**, 2536−2544. (h) Ochiai, M.; Iwaki, S.; Ukita, T.; Matsuura, Y.; Shiro, M.; Nagao, Y. *J. Am. Chem. Soc.* **1988**, *110*, 4606−4610. (i) Sauer, J.; Heldmann, D. K.; Range, K.-J.; Zabel, M. *Tetrahedron* **1998**, *54*, 12807−12822. (j) Kemmer, M.; Biesemans, M.; Gielen, M.; Tiekink, E. R. T.; Willem, R. *J. Organomet. Chem.* **2001**, *634*, 55−60. (k) Ren, Y.; Jia, C.; Liang, P.; Yang, X.; Chen, H. *Synth. React. Inorg. Met. Org. Chem.* **2003**, *33*, 1115−1123. (l) Harrison, W. T. A.; Howie, R. A.; Jaspars, M.; Wardell, S. M. S. V.; Wardell, J. L. *Polyhedron* **2003**, *22*, 3277−3288.

(17) Kolb, U.; Drager, M.; Jousseaume, B. *Organometallics* **1991**, *10*, 2737−2742.

(18) (a) Cox, P. J.; Doidge-Harrison, S. M. S. V.; Nowell, I. W.; Howie, R. A.; Randall, A. P.; Wardell, J. L. *Inorg. Chim. Acta* **1990**, *172*, 225−232. (b) Howie, R. A.; Wardell, J. L.; Zanetti, E.; Cox, P. J.; Doidge-Harrison, S. M. S. V. *J. Organomet. Chem.* **1992**, *431*, 27−40.

(19) Cox, P. J.; Doidge-Harrison, S. M. S. V.; Nowell, I. W.; Howie, R. A.; Wardell, J. L.; Wigzell, J. M. *Acta Crystallogr.* **1990**, *C46*, 1015−1017.

(20) Munguia, T.; Pavel, I. S.; Kapoor, R. N.; Cervantes-Lee, F.; Párkányi, L.; Pannell, K. H. *Can. J. Chem.* **2003**, *81*, 1388−1397.

(21) (a) Jastrzebski, J. T. B. H.; Grove, D. M.; Boersma, J.; Van Koten, G.; Ernsting, J. M. *Magn. Reson. Chem.* **1991**, *29*, S25−S30. (b) Jastrzebski, J. T. B. H.; Van Koten, G.; Knaap, C. T.; Schreurs, A. M. M.; Kroon, J.; Spek, A. L. *Organometallics* **1986**, *5*, 1551−1558.

(22) (a) Van Koten, G.; Jastrzebski, J. T. B. H.; Noltes, J. G.; Pontenagel, W. M. G. F.; Kroon, J.; Spek, A. L. *J. Am. Chem. Soc.* **1978**, *100*, 5021−5028. (b) Van Koten, G.; Noltes, J. G.; Spek, A. L. *J. Organomet. Chem.* **1976**, *118*, 183−189. (c) Rippstein, R.; Kickelbick, G.; Schubert, U. *Monatsh. Chem.* **1999**, *130*, 385−399.

(23) (a) Ettorre, R.; Marton, D.; Nodari, L.; Russo, U. *J. Organomet. Chem.* **2006**, *691*, 805−808. (b) Girasolo, M. A.; Schillaci, D.; Di Salvo, C.; Barone, G.; Silvestri, A.; Ruisi, G. *J. Organomet. Chem.* **2006**, *691*, 693−701. (c) Bhatti, M. H.; Ali, S.; Huma, F.; Shahzadi, S. *Turk. J. Chem.* **2005**, *29*, 463−476. (d) Barbieri, R.; Musmeci, M. T. *J. Inorg. Biochem.* **1988**, *32*, 89−108. (e) Barbieri, R.; Silvestri, A. *J. Inorg. Biochem.* **1991**, *41*, 31−35. (f) Domazetis, G.; Magee, R. J.; James, B. D. *J. Organomet. Chem.* **1979**, *173*, 357−376.

(24) (a) Harris, R. K.; Packer, K. J.; Ream, P. *Chem. Phys. Lett.* **1985**, *115*, 16−18. (b) Ruzicka, A.; Jambor, R.; Brus, J.; Cisarova, I.; Holecek, J. *Inorg. Chim. Acta* **2001**, *323*, 167−170. (c) Geller, J. M.; Wosnick, J. H.; Butler, I. S.; Gilson, D. F. R.; Morin, F. G.; Belanger-Gariepy, F. *Can. J. Chem.* **2002**, *80*, 813−820.

(25) Harris, R. K.; Sebald, A.; Furlani, D.; Tagliavini, G. *Organometallics* **1988**, *7*, 388−394.

(26) Geller, J. M.; Butler, I. S.; Gilson, D. F. R.; Wharf, I.; Bélanger-Gariépy, F. *Can. J. Chem.* **2003**, *81*, 1187−1195.

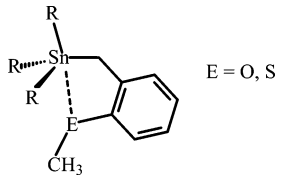

Figure 3. *o*-EMe-benzyl-chloride ligand used to bring E within proximity of Organotin moiety.

type B using *o*-thiomethylbenzyl[20,27] or *o*-methoxybenzyl groups to bring tin within proximity of the chalcogen atom, i.e., (*o*-MeE-C_6H_4)$CH_2SnPh_{3-n}Cl_n$, E = O, $n = 0$ (**1**), $n = 1$ (**2**), $n = 2$ (**3**); E = S, $n = 0$ (**4**), $n = 1$ (**5**), $n = 2$ (**6**), Figure 3. This series provides the capacity to observe the effect of changing the Lewis acidity at tin upon the nature of the intramolecular interactions and relating the single-crystal structures to the solid-state NMR spectroscopic data their relationship with the corresponding data obtained in solution.

Experimental Section

Synthesis. All manipulations were carried out under a nitrogen atmosphere using standard Schlenk line techniques. Reagent grade tetrahydrofuran (THF) was dried and distilled under nitrogen from a sodium benzophenone ketyl solution; benzene and hexanes were dried and distilled from Na ribbon. Triphenyltinchloride was purchased from Gelest; 2-methoxybenzyl chloride and 1 M HCl in diethyl ether were purchased from Aldrich; 2-thiomethylbenzyl chloride was synthesized by published methods as was **4**.[20,27] The new polymorph, **4′** was formed by fast crystallization upon cooling from a hot hexanes/dichloromethane (1:1) solution. Solution NMR spectra of all compounds were recorded on a Bruker 300 MHz spectrometer in $CDCl_3$. Elemental analyses were performed by Galbraith Laboratories.

X-ray Diffraction. Crystals suitable for X-ray diffraction were obtained for compounds **1**−**3** and **4′**−**6** from a hexanes/dichloromethane solution. Crystals of **1**, **2**, **3**, **4**, **5**, and **6** were mounted on glass fibers in random orientation. The X-ray intensity data were measured on a Bruker SMART APEX CCD area detector system equipped with a graphite monochromator and a Mo Kα fine-focus sealed tube ($\lambda = 0.71073$ Å). Frames were collected with a scan width of 0.30° in ω and an exposure time of 10 s/frame. The frames were integrated with the Bruker SAINT software package using a narrow-frame integration algorithm. Analysis of the data showed negligible decay during data collection. No absorption correction was applied. The structures were solved and refined using the Bruker SHELXTL (Version 6.1012) software package (full-matrix least-squares on F^2). The corresponding experimental parameters for each compound are summarized in Table 1.

Solid-State NMR. The ^{119}Sn solid-state spectra for compounds **1**−**3** and **4**−**6** were recorded at 93.3 MHz using a Bruker 250 MHz spectrometer. Spectra for compounds **4** (mixture) were also recorded on a Varian Unityplus 300 MHz spectrometer recorded at 111.9 MHz. The spectra were obtained under ^{119}Sn−^{1}H cross polarization (CP), magic angle spinning (MAS), and high powered proton decoupling. Zirconia or silicon nitride rotors (7.5 mm o.d.) with Kel-F caps were packed with 100−300 mg of compound, depending on the sample, and a Teflon spacer was used when the amount of sample available was insufficient for efficient packing. At least two different spin rates, between 2000 and 7000 Hz, were used to determine the isotropic peak, δ_{iso}. Chemical shifts are reported with respect to external tetramethyl tin, using the solid-state chemical shift of tetracyclohexyltin (−97.3 ppm) as a standard.[28] Tetracyclohexyltin was also used to set the Harman−Hahn match and the parameters for cross polarization. The centers of gravity for compounds **2**, **3**, **5**, and **6** were extracted using Dmfit,[29] and shielding tensor analysis was accomplished using the method of Herzfeld and Berger[30] and the computational program HBA version 1.4.4.[31]

Synthesis of (*o*-MeOC$_6$H$_4$)CH$_2$SnPh$_3$ (1). *o*-(Methoxy)benzyl-chloride (2.25 g, 14.37 mmol) was added dropwise to a mixture of Ph_3SnCl (5.54 g, 14.37 mmol) and Mg turnings (0.349 g, 14.37 mmol) in THF (10 mL) at 0 °C. The reaction mixture was kept at 0 °C and allowed to stir until all the Mg had been consumed, 16 h. The solvent was removed under reduced pressure, and the product was extracted with a hexanes/dichloromethane solution (10:1) and filtered. The crude material was recrystallized from a hexane/dichloromethane solution (10:1) and cooled to −20 °C, to yield **1** as a white solid. Yield: 3.4 g (68%); mp 60−62 °C. ^{1}H NMR ($CDCl_3$) δ 2.93 (2H, s, CH_2−Sn, $^2J(^{117/119}Sn-C^1H_2) = 13.23/32.45$ Hz), 3.34 (3H, s, O−CH_3), 7.47−7.30 (19H, m, Ph). ^{13}C NMR ($CDCl_3$) δ 16.1 (CH_2Sn, $^2J(^{13}C-^{117/119}Sn) = 171.09/179.13$ Hz), 54.71 (O−CH_3), 109.9, 120.9, 125.8 (C_{ipso}−C), 128.7 (*m*-Ph−Sn, $^2J(^{13}C-^{119}Sn) = 23.4$ Hz), 129.0, 129.1 (*p*-Ph−Sn, $^2J(^{13}C-^{119}Sn) = 5.02$ Hz), 129.6, 137.3 (*o*-Ph−Sn, $^2J(^{13}C-^{117/119}Sn) = 17.62/38.02$ Hz), 140.0 (*ipso*-Ph−Sn, $^2J(^{13}C-^{117/119}Sn) = 234.22/245.17$ Hz), 156.20 (C_{ipso}−O). ^{119}Sn NMR ($CDCl_3$) δ −114.8. Anal. Calcd for $C_{26}H_{24}OSn$: C 66.28, H 5.13. Found: C 66.12, H 5.29.

Synthesis of (*o*-MeOC$_6$H$_4$)CH$_2$Ph$_2$SnCl (2). A solution of **1** (3 g, 6.36 mmol) in 15 mL of dried benzene was added dropwise to a solution of hydrogen chloride (1.0 M in diethyl ether, 6.36 mL, 6.36 mmol). After 15 min, the reaction was complete and the solvent was removed under reduced pressure. The crude material was recrystallized from hot hexane and cooled to −20 °C to yield **2**: 2.0 g (75%); mp 116−117 °C. ^{1}H NMR ($CDCl_3$) δ 3.05 (2H, s, CH_2−Sn, $^2J(^{117/119}Sn-C^1H_2) = 19.92/42.14$ Hz); 3.46 (3H, s, O−CH_3), 7.65−6.70 (14H, m, Ph). ^{13}C NMR ($CDCl_3$) δ 20.9 (CH_2-Sn), $^2J(^{13}C-^{117/119}Sn) = 219.45/230.95$ Hz), 54.9 (O−CH_3), 109.9, 121.8, 127.05, 127.14 (C_{ipso}−C), 128.9 (*m*-Ph−Sn, $^2J(^{13}C-^{119}Sn) = 30.2$ Hz), 130.0 (*p*-Ph−Sn, $^2J(^{13}C-^{119}Sn) = 6.6$ Hz), 130.2, 135.8 (*o*-Ph−Sn, $^2J(^{13}C-^{117/119}Sn) = 22.80/37.72$ Hz), 139.8 (*ipso*-Ph−Sn, $^2J(^{13}C-^{117/119}Sn) = 289.2/302.7$ Hz), 155.20 (C_{ipso}−O). ^{119}Sn NMR ($CDCl_3$) δ −41.4. Anal. Calcd for $C_{20}H_{19}OSnCl$: C 55.93, H 4.46. Found: C 55.65, H 4.57.

The related chlorotin compounds **3**, **5**, and **6** followed the same general procedure outlined above.

(*o*-MeOC$_6$H$_4$)CH$_2$PhSnCl$_2$ (3). 1.08 g (80%); mp 79−80 °C. ^{1}H NMR ($CDCl_3$) δ 3.17 (2H, s, CH_2−Sn, $^2J(^{117/119}Sn-C^1H_2) = 15.75/41.43$ Hz); 3.66 (3H, s, O−CH_3); 7.55−6.70 (9H, m, Ph). ^{13}C NMR ($CDCl_3$) δ 27.3 (CH_2Sn), $^2J(^{13}C-^{117/119}Sn) = 214.45/239.95$ Hz), 55.4 (O−CH_3), 110.3, 122.39, 124.44, 128.5 (C_{ipso}−C), 129.7 (*m*-Ph−Sn, $^2J(^{13}C-^{119}Sn) = 34.2$ Hz), 130.6, 131.5 (*p*-Ph−Sn, $^2J(^{13}C-^{119}Sn) = 6.2$ Hz), 134.88 (*o*-Ph−Sn, $^2J(^{13}C-^{117/119}Sn) = 22.80/37.72$ Hz), 140.41 (*ipso*-Ph−Sn, $^2J(^{13}C-^{117/119}Sn)$

(27) Traynelis, V. J.; Borgnaes, D. M. *J. Org. Chem.* **1972**, *37*, 3824−3826.

(28) Bryce, D. L.; Bernard, G. M.; Gee, M.; Lumsden, M. D.; Eichele, K.; Wasylishen, R. E. *Can. J. Anal. Sci. Spectrosc.* **2001**, *46*, 46−82.

(29) Massiot, D.; Fayon, F.; Capron, M.; King, I.; Le Calvé, S.; Alonso, B.; Durand, J.-O.; Bujoli, B.; Gan, Z.; Hoatson, G. *Magn. Reson. Chem.* **2002**, *40*, 70−76.

(30) Herzfeld, J.; Berger, A. E. *J. Chem. Phys.* **1980**, *73*, 6021−6030.

(31) Eichele, K.; Wasylishen, R. E. *HBA*, 1.4.4; Dalhousie University: Halifax, Canada, 2001.

Table 1. Crystal Data and Structure Refinement for Crystal Structure Analysis of Compounds **1**−**6**

	1	**2**	**3**	**4′**	**5**	**6**
empirical formula	$C_{26}H_{24}OSn$	$C_{20}H_{19}ClOSn$	$C_{14}H_{14}Cl_2OSn$	$C_{26}H_{24}SSn$	$C_{20}H_{19}ClS\ Sn$	$C_{14}H_{14}Cl_2SSn$
fw (g/mol)	471.14	429.49	387.84	487.20	445.55	403.90
temp (K)	293(2)	296(2)	296(2)	123(2)	293(2)	296(2)
λ (Å)	0.71073	0.71073	0.71073	0.71073	0.71073	0.71073
cryst syst	orthorhombic	monoclinic	monoclinic	monoclinic	monoclinic	orthorhombic
space group	*Pna*21	$P2_1/c$	$P2_1/c$	$P2_1/c$	$P2_1/c$	$P2(1)2(1)2(1)$
a (Å)	16.9091(15)	8.4114(13)	7.7795(13)	19.066(4)	8.8031(6)	9.6460(10)
b (Å)	15.8687(14)	26.655(4)	19.780(3)	14.766(3)	27.5903(18)	9.656(2)
c (Å)	8.1595(7)	8.7420(13)	9.8816(16)	7.9109(17)	8.5728(6)	16.592(3)
α (°)	90	90	90	90	90	90
β (°)	90	109.885(2)	94.183(3)	98.743(5)	113.8220(10)	90
γ (°)	90	90	90	90	90	90
V Å^3	2189.4(3)	1843.1(5)	1516.5(4)	2201.3(8)	1904.8(2)	1545.4(5)
Z	4	4	4	4	4	4
D_x(Mg/m^3)	1.429	1.548	1.699	1.470	1.554	1.736
μ (mm^{-1})	1.180	1.533	2.023	1.264	1.588	2.114
F (000)	952	856	760	984	888	792
cryst size (mm^3)	0.60 × 0.40 × 0.40	0.96 × 0.48 × 0.42	0.45 × 0.30 × 0.03	0.20 × 0.08 × 0.04	0.16 × 0.12 × 0.06	0.40 × 0.30 × 0.10
θ range for data collection (°)	1.76−23.27	1.53−28.28	2.31−28.20	1.08−28.28	1.48−28.26	2.44−25.04
index ranges	$-18 \le h \le 8$	$-10 \le h \le 10$	$-10 \le h \le 10$	$-19 \le h \le 24$	$-11 \le h \le 10$	$-11 \le h \le -11$
	$-15 \le k \le 17$	$-34 \le k \le 35$	$-22 \le k \le 25$	$-18 \le k \le 19$	$-36 \le k \le 33$	$-11 \le k \le 11$
	$-8 \le l \le 9$	$-11 \le l \le 11$	$-10 \le l \le 12$	$-10 \le l \le 8$	$-11 \le l \le 11$	$-19 \le l \le 19$
reflns collected	9445	19 465	9435	13 692	11 995	3634
independent reflns	3120	4296	3511	5116	4411	2741
R(int)	0.0218	0.0251	0.0222	0.0453	0.0188	0.0284
data/ restraints/ params	3120/1/254	4296/0/208	3511/0/164	5116/0/254	4411/0/209	2741/0/164
GOF on F^2	1.067	1.279	1.040	1.034	0.425	0.986
final *R* indices [$I > 2\sigma(I)$]	R1 = 0.0221	R1 = 0.0406	R1 = 0.0284	R1 = 0.0522	R1 = 0.0292	R1 = 0.0376
	wR2 = 0.0584	wR2 = 0.0802	wR2 = 0.0731	wR2 = 0.0991	wR2 = 0.0764	wR2 = 0.0997
R indices (all data)	R1 = 0.0226	R1 = 0.0452	R1 = 0.0344	R1 = 0.0791	R1 = 0.0382	R1 = 0.0381
	wR2 = 0.0587	wR2 = 0.0816	wR2 = 0.0763	wR2 = 0.1099	wR2 = 0.0919	wR2 = 0.1005
largest diff. peak and hole (e·A^{-3})	0.194 and −0.354	0.588 and −0.882	0.589 and −0.521	0.980 and −0.682	0.491 and −0.289	1.506 and −1.040

= 275.2/314.7 Hz), 155.0 (C_{ipso}−O). ^{119}Sn NMR ($CDCl_3$) δ −32.69. Anal. Calcd for $C_{14}H_{14}OSnCl_2$: C 43.35, H 3.64. Found: C 43.56, H 3.97.

(*o*-CH$_3$SC$_6$H$_4$)CH$_2$SnPh$_2$Cl, (5). 0.35 g (30%); ^{1}H NMR ($CDCl_3$): δ 2.0 (3H, s, S−CH_3); J(^{119}Sn−^{1}H) 40.04 Hz; 3.16 (2H, s, CH_2−Sn); J(^{119}Sn−^{1}H) 79.81 Hz; 7.6−7.1 (9H, m, Ph). ^{13}C NMR ($CDCl_3$): δ 16.6 (SCH_3); 29.3 (CH_2−Sn); 139.7; 135.7; J($^{119/117}$Sn$_{ave}$−^{13}C) 44.67 Hz; 129.7 J($^{119/117}$Sn$_{ave}$−^{13}C) 13.6 Hz; 128.6 J($^{119/117}$Sn$_{ave}$−^{13}C) 62.3 Hz; 138.6 (C_{ipso}−CH_2Sn); 133.4 (C_{ortho}−SCH_3); 128.9; 126.9; 126.8; 126.4 ^{119}Sn NMR ($CDCl_3$): δ −46.3. Anal. Calcd for $C_{20}H_{19}SCl$: C, 53.91; H, 4.30. Found: C, 53.90; H, 4.20.

***o*-(CH$_3$SC$_6$H$_4$)CH$_2$SnPhCl$_2$, (6).** 0.3 g (32%); ^{1}H NMR ($CDCl_3$): δ 2.40 (3H, s, S−CH_3); 3.30 (2H, s, CH_2−Sn); 7.2−7.7 (14H, m, Ph) ^{13}C NMR ($CDCl_3$): δ 17.7 (SCH_3); 35.7 (CH_2−Sn); 141.0 (C_{ipso}−CH_2Sn); 137.5 (C_{ortho}−SCH_3); 135.8; 134.3 J($^{119/117}$Sn$_{ave}$−^{13}C) 59.6 Hz; 130.8 J($^{119/117}$Sn$_{ave}$−^{13}C) 17.4 Hz; 129.4 J($^{119/117}$Sn$_{ave}$−^{13}C) 45.1 Hz; 129.1; 127.6; 127.5; 127.3; ^{119}Sn NMR ($CDCl_3$): δ −48.5. Anal. Calcd for $C_{14}H_{14}Cl_2SSn$: C, 41.63; H, 3.49. Found: C, 41.47; H, 3.69.

Results and Discussion

Synthesis. The synthesis of compounds **1**−**6** followed the scheme outlined below in eqs 1−3, E = O, S, using published general procedures.[20]

$$Ph_3SnCl + (o\text{-}MeEC_6H_4)CH_2MgCl \rightarrow Ph_3SnCH_2(C_6H_4\text{-}o\text{-}EMe) + MgCl_2 \quad (1)$$

$$Ph_3SnCH_2(C_6H_4\text{-}o\text{-}EMe) + HCl/Et_2O \rightarrow ClPh_2SnCH_2(C_6H_4\text{-}o\text{-}EMe) + PhH \quad (2)$$

$$ClPh_2SnCH_2(C_6H_4\text{-}o\text{-}EMe) + HCl/Et_2O \rightarrow Cl_2PhSnCH_2(C_6H_4\text{-}o\text{-}EMe) + PhH \quad (3)$$

In the case of the chemistry outlined in equivalent 2, exactly 1 equiv of 1 M HCl/ether must be added to ensure that no mixtures of monochlorotin and dichlorotin compounds are obtained. In this regard, the use of the HCl/ether reagent is particularly useful since it permits exactly stoichiometric reaction conditions as compared to the direct use of HCl gas. The progress of the chlorination reactions was conveniently monitored by taking aliquots of the reaction solution and using ^{119}Sn NMR spectroscopy (without locking) **1** → **2** → **3** (−114.9 → −41.4 → −32.6 ppm) and **4** → **5** → **6** (−115.5 → −46.4 → −48.5 ppm).

Crystal Structures. X-ray quality crystals of compounds **1**−**6** were obtained and used to determine the molecular structures. Figures 4−9 represent molecular structures of compounds **1**−**3** and **4′**−**6**, and selected bond lengths and angles are given in Table 2. The structure of compound **4** has been previously reported;[20] however, during the present study, arising from the solid state ^{119}Sn NMR spectra of **4** (vide infra), we observed and isolated a second crystalline form, **4′**, whose structure is reported here, Figure 7.

For the series of compounds **1**, **2**, **3**, **4**, **4′**, **5**, and **6**, the various Sn−C (phenyl) bond lengths fall within the sum of the covalent radii (2.15 Å) for tin and carbon[32] and are similar to other organotin−phenyl bond lengths, e.g., Ph_4Sn, 2.144-(14) Å.[33] Similarly, the Sn−C (benzyl) bond distances, within the experimental errors, exhibit no significant variations.

One of the objectives of this study was to determine the extent of intramolecular Sn−E interactions as a function of

(32) O'Keefe, M.; Brese, N. E. *J. Am. Chem. Soc.* **1991**, *113*, 3226−3229.
(33) Chieh, P. C. *J. Chem. Soc., A* **1971**, 3243−3245. Chieh, P. C. *J. Chem. Soc., Dalton Trans.* **1972**, 1207−1208.

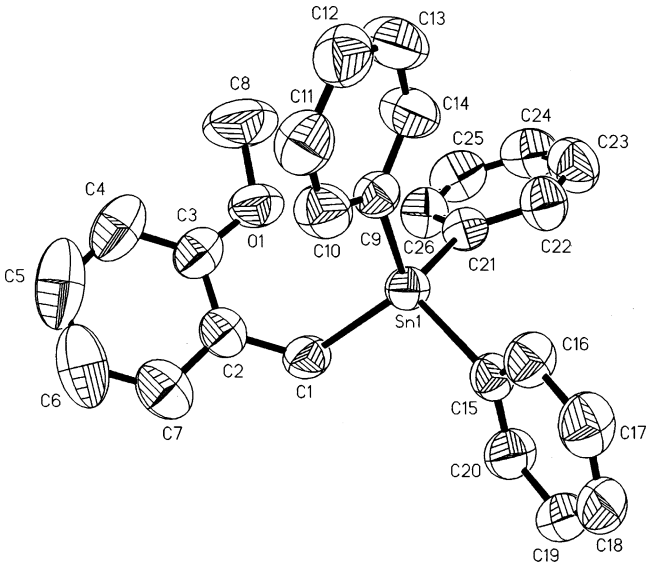

Figure 4. ORTEP diagram of compound **1**.

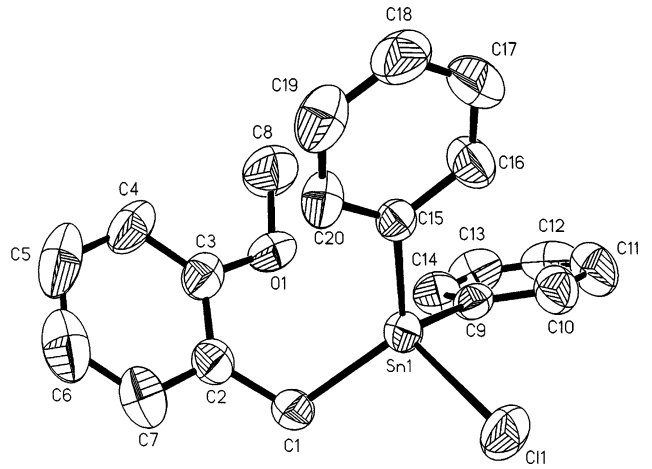

Figure 5. ORTEP diagram of compound **2**.

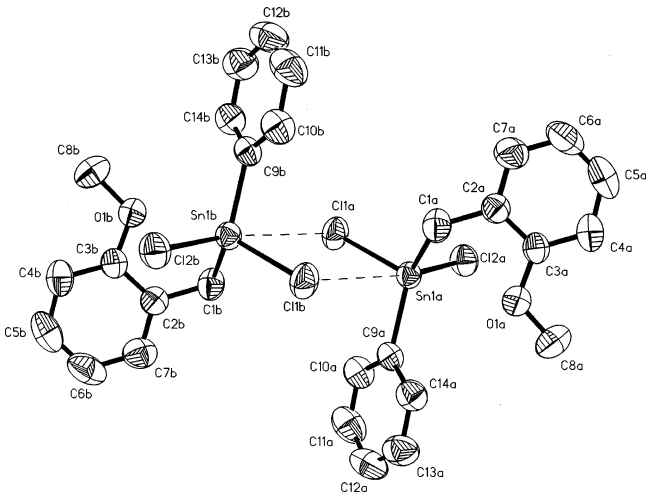

Figure 6. ORTEP diagram of compound **3** illustrating Sn−Cl zigzag intermolecular interaction.

progressively changing the Lewis acidity of the central tin atom. In the series of E = S the Sn−S distances are 3.973 (**4′**), 3.699 and 3.829 (**4**)[20], 3.062 (**5**), and 2.99 Å (**6**). Thus, a significant increase in the intramolecular Sn−S interaction

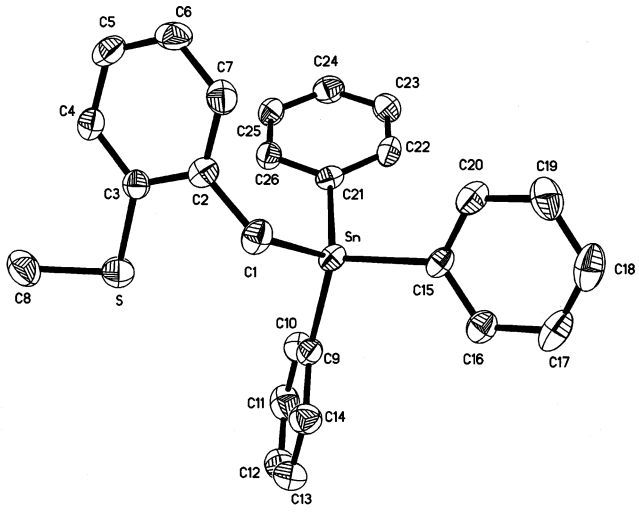

Figure 7. ORTEP diagram of compound **4′**.

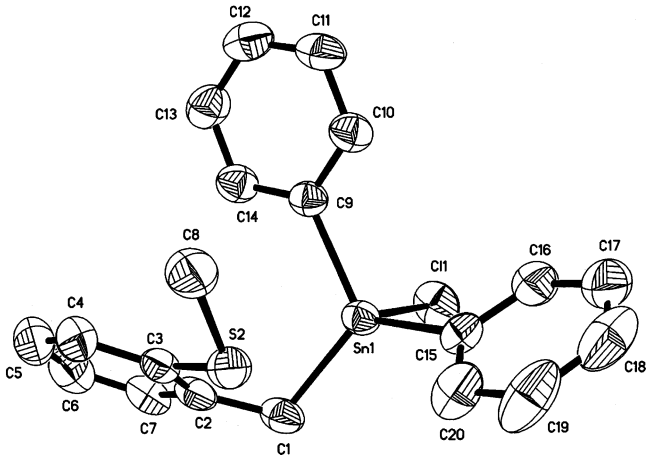

Figure 8. ORTEP diagram of compound **5**.

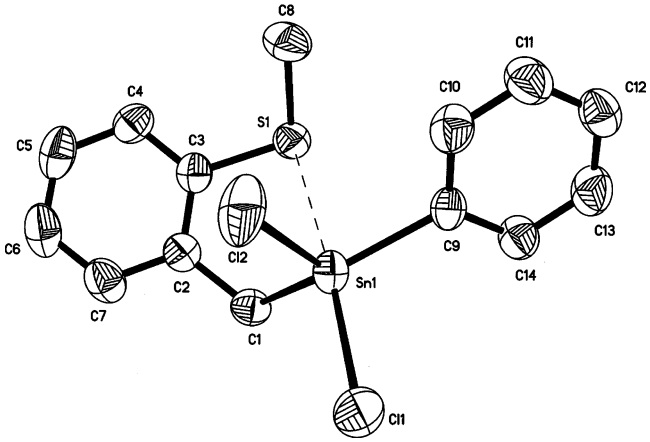

Figure 9. ORTEP diagram of compound **6**.

is noted upon replacing the phenyl groups by chlorine in response to the increasing Sn Lewis acidity and represents a change from ∼90% to 71% of the sum of the Sn and S van der Waals radii. In the Cl-substituted compounds **5** and **6**, the intramolecular Sn−S bonding is transoid to the Sn−Cl bond with Cl−Sn−S angles of 168° and 167°, respectively.

Table 2. Selected Bond Lengths (Å) and Angles (deg) for the Following Compounds

	1 E = O	**2** E = O	**3** E = O	**4′** E = S	**5** E = S	**6** E = S
E−Sn	3.07	2.767	2.898	3.973	3.062	2.994
E−C(3)	1.367(5)	1.384(5)	1.372(3)	1.756(4)	1.765(4)	1.770(5)
E−C(8)	1.406(5)	1.425(5)	1.426(3)	1.792(5)	1.788(4)	1.786(6)
Sn−C(1)	2.158(3)	2.132(4)	2.130(3)	2.168(4)	2.153(3)	2.132(5)
Sn−C(9)	2.139(3)	2.130(3)	2.111(3)	2.134(4)	2.137(3)	2.123(5)
Sn−C(15)	2.158(3)	2.137(3)	−	2.131(4)	2.132(3)	−
Sn−C(21)	2.147(3)	−	−	2.136(4)	−	−
Sn−Cl(1)	−	2.3991(10)	2.3722(8)	−	2.4130(9)	2.4042(14)
Sn−Cl(2)	−	−	2.3600(8)	−	−	2.3504(15)
C(2)−C(1)−Sn	115.0(2)	110.5(2)	110.63(17)	116.0(3)	110.7(2)	112.1(3)
C(9)−Sn−C(1)	116.15(12)	117.53(15)	129.66(11)	113.33(18)	117.08(13)	140.15(18)
C(9)−Sn−C(21)	108.09(12)	−	−	107.17(16)	−	−
C(15)−Sn−C(1)	107.13(11)	119.23(14)	−	104.11(15)	121.93(15)	−
C(15)−Sn−C(9)	103.82(12)	111.54(13)	−	110.28(16)	111.49(13)	−
C(15)−Sn−C(21)	112.44(12)	−	−	109.31(16)	−	−
C(21)−Sn−C(1)	109.22(13)	−	−	112.62(16)	−	−
C(1)−Sn−Cl(1)	−	103.57(11)	106.43(8)	−	101.32(10)	100.17(13)
C(9)−Sn−Cl(1)	−	101.23(10)	105.00(7)	−	99.60(9)	102.29(13)
C(15)−Sn−Cl(1)	−	99.61(9)	−	−	100.00(10)	−
C(1)−Sn−Cl(2)	−	−	108.28(8)	−	−	106.27(16)
C(9)−Sn−Cl(2)	−	−	105.97(7)	−	−	102.99(13)
Cl(1)−Sn−Cl(2)	−	−	96.61(3)	−	−	97.35(7)
C(2)−C(3)−E	114.0(3)	113.2(3)	114.6(2)	118.3(3)	115.5(3)	116.5(4)
C(3)−E−C(8)	117.6(4)	117.6(3)	117.4(2)	103.3(2)	104.0(2)	103.3(3)
C(4)−C(3)−E	124.8(4)	125.1(4)	124.9(3)	122.6(3)	123.1(3)	122.2(4)
C(10)−C(9)−Sn	122.9(3)	120.5(3)	119.4(2)	120.3(3)	119.4(2)	117.7(4)
C(14)−C(9)−Sn	120.2(3)	120.8(3)	121.3(2)	121.7(3)	122.4(2)	123.3(4)
C(16)−C(15)−Sn	119.9(2)	117.5(3)	−	123.0(3)	119.9(3)	−
C(20)−C(15)−Sn	122.2(2)	124.5(3)	−	119.4(3)	122.3(3)	−
C(22)−C(21)−Sn	121.5(3)	−	−	120.6(3)	−	−
C(26)−C(21)−Sn	121.5(3)	−	−	121.7(3)	−	−

These intramolecular Sn−E interactions have consequences on the geometry at Sn. The transition from tetrahedral to trigonal bipyramidal (tbp) can be monitored by looking at the difference between the sum of the "equatorial" angles and the sum of the "axial" angles, Figure 10.[12,13,15,17] A tetrahedral geometry would have "axial" angles which would add up to 328.5° (Σax) and "equatorial" angles that would also add up to 328.5° (Σeq), i.e., (Σeq − Σax) = 0°. For a tbp geometry, (Σax) = 270° and (Σeq) = 360°; therefore, (Σeq − Σax) = 90°. Thus, progressively greater (Σeq − Σax) values are associated with the more tbp structures.

The bond orders (BO) of the Sn−E bonds as defined in eq 4 have been used as a measure of the strength of such interactions.[15,19,34]

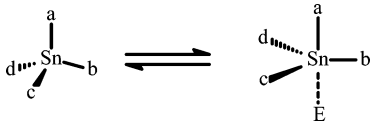

Figure 10. Transition from tetrahedral geometry to trigonal bipyramid. Atoms b, c, and d become "equatorial", and atoms a and E become axial.

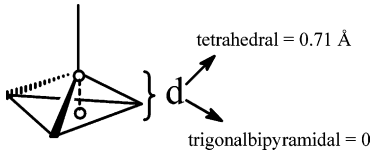

Figure 11. ΔSn_{plane} used to help map the transition from tetrahedral to trigonal bipyramidal in compounds **1**−**3**, and **4′**−**6**.

$$BO = d(Sn{-}E_{ave}) + 1 - d(Sn{-}E) \quad (4)$$

Non-zero values can be related to the strength of the E−S interaction.

The deviation of the Sn atom from the centroid of the plane created by the three equatorial atoms in the tbp structure should be zero, Figure 11. In a general tetrahedral structure, such a value would be 0.71 Å.[13,17] The degree to which the Sn atom deviates from the centroid of the plane between 0 and 0.71 can also help map the progression from tetrahedral to tbp. Table 3 summarizes the various data from the methods above to monitor the path from tetrahedral to tbp taken for compounds **4** (**4′**), **5**, and **6**. In terms of the Σeq − Σax term the transformation **4** (**4′**) → **5** → **6** the values are 5° (average) → 50° → 50°, respectively; the BO values are −0.43 (average) → 0.33 → 0.41, respectively, and the distance of the tin atom from the centroid of the equatorial groups are 0.675 Å → 0.39 Å → 0.37 Å, respectively. These data generally trend together; however, they are not precisely equivalent in terms of indicating the Sn−S interaction. Clearly, the angular term does not reflect the greater Sn−S interaction in **6**, suggesting that a great deal of flexibility exists in this class of compound.

A closer examination of the structure of **6** reveals an intermolecular Sn−Cl2−H8 hydrogen bond of 2.847 Å, Figure 12. Metal-bound chlorine has been shown to be a good hydrogen bond acceptor.[35,36] The sum of the Van der Waals radii for H and Cl is 2.95 Å,[35,37] and in general, M−Cl−H−C contacts come in three lengths: short ≤2.52

(34) Dräger, M. *Z. Anorg. Allg. Chem.* **1976**, *423*, 53−66.
(35) Aullón, G.; Bellany, D.; Brammer, L.; Burton, E. A.; Orpen, A. G. *Chem. Commun.* **1998**, 653−654.

Table 3. Summary Data Obtained Used to Analyze the Pathway from Tetrahedral to Trigonal Bipyramidal for Compounds **1**−**6**

compd	Sn−E (Å)	equatorial angles (deg)	Σeq (deg)	axial angles(deg)	Σax (deg)	Σeq − Σax (deg)	BO	ΔSn_{plane}
1	3.07	C21−Sn−C1 C9−Sn−C21 C9−Sn−C1	333.46	C1−Sn−C15 C21−Sn−C15 C9−Sn−C15	323.39	10.07	−0.07	0.652
2	2.76	C1−Sn−C15 C9−Sn−C15 C1−Sn−C9	348.30	Cl−Sn−C9 Cl−Sn−C1 Cl−Sn−C15	304.41	43.89	0.24	0.431
3 Sn−O	2.92	C1−Sn−Cl2 Cl2−Sn−C9 C1−Sn−C9	343.91	Cl−Sn−C1 Cl−Sn−C9 Cl−Sn−Cl2	308.04	35.87	0.08	0.502
Sn−Cl	3.488	Cl−Sn−C1 Cl−Sn−C9 C1−Sn−C9	341.09	Cl2−Sn−C9 C1−Sn−Cl2 Cl−Sn−Cl2	310.81	30.28	−0.128	
4 a	3.69	C21−Sn−C1 C9−Sn−C21 C9−Sn−C1	333.4	C1−Sn−C15 C21−Sn−C15 C9−Sn−C15	323.3	10.1	−0.29	0.657
b	3.82	C21−Sn−C1 C9−Sn−C21 C9−Sn−C1	325.7	C1−Sn−C15 C21−Sn−C15 C9−Sn−C15	331.1	−5.4	−0.42	0.687
4′	3.973	C1−Sn−C9 C1−Sn−C21 C21−Sn−C9	333.12	C1−Sn−C15 C9−Sn−C15 C21−Sn−C15	323.7	9.42	−0.573	
5	3.062	C1−Sn−C15 C9−Sn−C15 C1−Sn−C9	350.5	Cl−Sn−C9 Cl−Sn−C1 Cl−Sn−C15	300.92	49.58	0.338	0.387
6	2.99	C1−Sn−Cl2 Cl2−Sn−C9 C1−Sn−C9	349.41	Cl−Sn−C1 Cl−Sn−C9 Cl−Sn−Cl2	299.81	49.6	0.41	0.366

Å, intermediate 2.52−2.95 Å, and long 2.95−3.15 Å.[35] The Cl2−H8 distance in **6** of 2.847 Å is well within the Van der Waals radii and is considered intermediate with the Sn−Cl2−H8 and Cl2−H8−C8 angles, 141.05° and 141.47°, respectively. Typical M−Cl−H angles can range as low as 90−130° but can reach as high as 180° for short H−Cl distances.[36] This H8−Cl2 interaction perpetuates itself throughout the crystal array, forming chains with a H8−Cl2−Sn−C−C−C−S−C−H−Cl2 backbone that continues in the *b* direction, Figure 12. The chains are singular, looping, neither intertwined nor helical. This interesting detail does not seem to interfere with the S−Sn intramolecular interaction of compound **6**; however, it could be a reason for the lack of further trigonal bipyramidal character of **6**, as noted by the Σeq − Σax term reported above.

The various oxygen-containing compounds exhibit similar, but distinctive, properties upon increasing the Cl content, i.e., **1** → **2** → **3**. Upon the transformation **1** → **2**, the Sn−O bond distance reduces from 3.07 to 2.767 Å, i.e. from 83% to 75% of the sum of the van der Waals radii paralleling the data for the S-containing compounds **4** and **5**. The Σeq − Σax term changes from 10° to 43°, and the distance of the tin atom from the centroid of the equatorial groups changes from 0.65 to 0.43 Å, all in accord with the previous data.

However, the structure of **3**, Figure 5, illustrates a complete change from all the previous structures in that the well-known capacity of organotin chlorides to exhibit intramolecular oligomerization via Sn−Cl interactions results in dimer formation. Thus, **3** exhibits an octahedral-type environment

(36) (a) Aakeröy, C. B.; Evans, T. A.; Seddon, K. R.; Pálinko, I. *New J. Chem.* **1999**, 145−152. (b) Balamurugan, V.; Hundal, M. S.; Mukherjee, R. *Chem. Eur. J.* **2004**, *10*, 1683−1690.

(37) Bondi, A. *J. Phys. Chem* **1964**, *68*, 441−451.

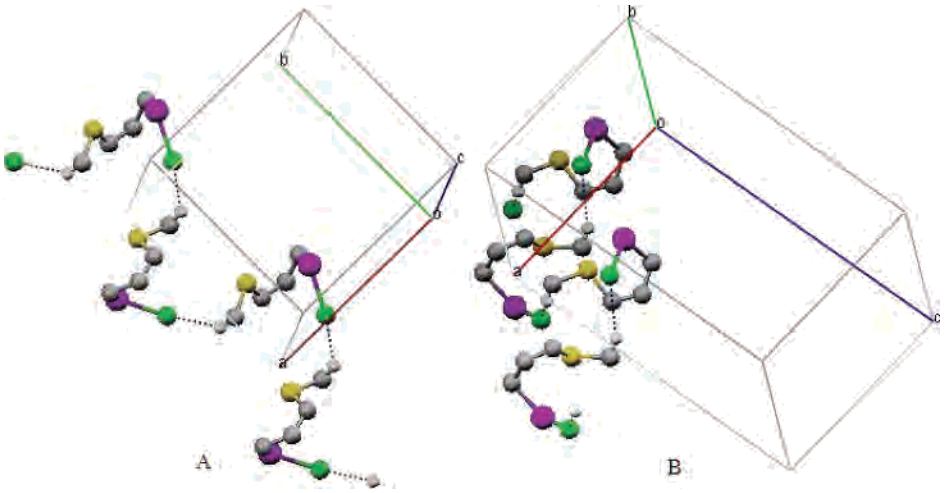

Figure 12. Two different views of the H8−Cl2−Sn intermolecular interaction discovered in **6**. Only the H8−Cl2−Sn−C−C−C−S−C−H−Cl2 backbone is shown for clarity. Green = Cl, purple = Sn, yellow = S, gray = C, white = H. Mercury 1.4 CCDC 2001-2005 was used to generate this view.

about Sn with both intramolecular Sn−O and intermolecular Sn−Cl bonding. As expected for the higher coordination number, the individual Sn−S and Sn−Cl interatomic distances are longer than would be the case for pentacoordination. Thus, the Sn−O distance of 2.92 Å is longer than that in **2** but still represents an interaction that is 79% of the sum of the two van der Waals radii. The two bridging Sn−Cl−Sn internuclear distances are 2.371(9) and 3.488 Å, typical of such dimeric structures with the other terminal Sn−Cl bond of 2.3604(9) Å being transoid to the weaker Sn−Cl bridging chlorine atom with a Cl−Sn−Cl angle of 171°. In a similar manner, the intramolecular Sn−S interaction is also transoid to the Sn−Cl bond, S−Sn−Cl angle of 168°. Our chalcogen−tin intramolecular interactions range from 83% to 75% for oxygen and 90% to 71% for sulfur. In contrast, amine analogues have intramolecular Sn−N interactions that run as low as 63% the sum of the van der Waals radii.[21−22]

Solid-State NMR. Solid-state NMR spectroscopy is a useful technique used to probe the structural details of compounds containing NMR active nuclei, often in systems where use of single-crystal X-ray diffraction is not possible.[38] Furthermore, whereas powder X-ray diffraction can also be used to study bulk properties, solid-state NMR has the advantage of utilizing spinning sidebands to offer more structural information.[30,39] Additionally, solid-state NMR spectroscopy is particularly useful in identifying polymorphs, or different crystal forms of powdered samples, a technique extremely useful to pharmaceutical studies.[40]

Polymorphism in organotin chemistry is not uncommon,[41,42] and the existence of new structural modifications can be revealed by solid-state NMR.[40,42] In the present case, when we obtained the ^{119}Sn CPMAS spectra for compound **4** we were surprised to see three isotropic peaks, Figure 13, two of equal intensity at −100.5 and −108.1 ppm and another, approximately three times more intense, at −115.5 ppm. This indicated a second crystal form, previously unreported, was present, **4′**. As noted above, we were able to grow X-ray-quality crystals and determine the differences in the Sn−S intramolecular interactions.

The chemical shift data for all compounds, both in solution ($CDCl_3$) and solid state are presented in Table 4. For the non-chlorinated compounds, $Ph_3Sn-CH_2(C_6H_4$-*o*-EMe), **1** and **4**, the ^{119}Sn CPMAS spectrum chemical shifts and the solution data are very similar, −102.4 and −114.9 (**1**) and −107.6 (average) and −115.5 ppm (**4**). These data represent $\delta\Delta$ ($\delta_{solid} - \delta_{solution}$) values of 12.5 (**1**) and 7.8 ppm (average, **4**), indicating that the mild E−Sn interactions and slightly distorted tetrahedral geometry is maintained in solution, as well as in the solid state. We have not been able to obtain a spectrum of the polymorph **4** alone, and as a result, its chemical shift tensor analysis, vide infra, is not included here. However, the monoclinic **4′** crystallized faster and therefore, a solid-state NMR spectrum of this polymorph, as a pure material, was obtained, Figure 14.

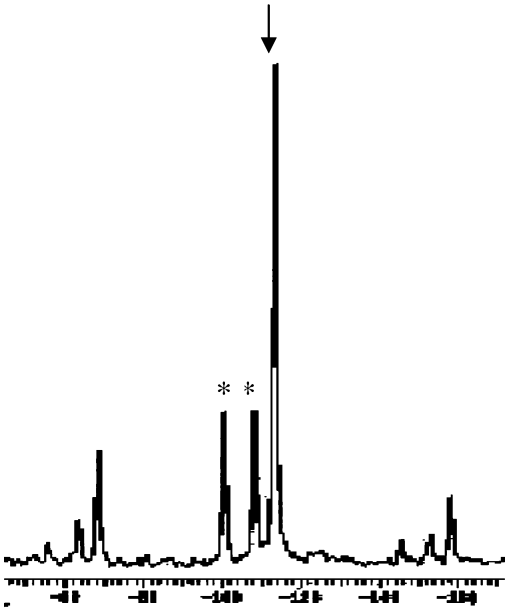

Figure 13. CPMAS ^{119}Sn spectra of a mixture of **4** (asterisks) and **4′** (arrow); spin rate 7000 Hz.

The ^{119}Sn CPMAS spectra of the mono- and dichloro tin compounds **2**, **3**, **5**, and **6** are illustrated in Figure 15. The isotropic peaks of the monochloro compounds **2** and **5** are complicated by secondary quadrupolar interactions between ^{119}Sn (spin 1/2) and $^{35/37}$Cl (spin 3/2) and show the characteristic splitting of a 1:1:2 triplet with approximate 2:1 spacing,[25,26] Figure 15. The $\delta\Delta$ ($\delta_{solid} - \delta_{solution}$) values of −15.1 (2) and −46.7 (5) are again on the low side of such possible variations, as noted by Harris et al.[24] These authors have suggested that $\delta\Delta$ of 10−15 ppm indicate no increase in association from the solution state to the solid state, moderate $\delta\Delta$ of ∼50 ppm can indicate an increase in coordination or minor changes in molecular geometry. Larger $\delta\Delta$ values were considered to be definite examples of increased coordination in the solid state compared to solution structures.[25] The chemical shift data for the new compounds are consistent with only small distinctions between the solution and solid-state structures for **1**, **2**, **4**, and **5**. This feature becomes important when considering the bioavailability of the monochloro compounds **2** and **5** since it is such intramolecular interactions that seem to be preserved in solution, which will effectively compete with intermolecular Sn−N or Sn−S interactions that serve as initiators of the biological activity of organotins.

Compound **3** with the intramolecular O−Sn and intermolecular Cl−Sn interactions (pseudo-octahedral) has an iso-

(38) Grindley, T. B.; Wasylishen, R. E.; Thangarasa, R.; Power, W. P.; Curtis, R. D. *Can. J. Chem.* **1992**, *70*, 205−217.
(39) (a) Harris, R. K.; Lawrence, S. E.; Oh, S.-W.; Das, V. G. K. *J. Mol. Struct.* **1995**, *347*, 309−320. (b) Hodgkinson, P.; Emsley, L. *J. Chem. Phys.* **1997**, *107*, 4808−4816.
(40) Portieri, A.; Harris, R. K.; Fletton, R. A.; Lancaster, R. W.; Threlfall, T. L. *Magn. Reson. Chem.* **2004**, *42*, 313−320.
(41) (a) Cunningham, D.; Firtear, P.; Molloy, K. C.; Zuckermann, J. J. *J. Chem. Soc. Dalton Trans.* **1983**, 1523−1527. (b) Lay, U.; Pritzhow, H.; Grützmacher, H. *J. Chem. Soc., Chem. Commun.* **1992**, 260−262. (c) Molloy, K. C.; Tagliavini, G.; Ganis, P.; Furlani, D. *Inorg. Chim. Acta* **1988**, *141*, 7−8. (d) Ng, S. W.; Rae, A. D. *Acta Cryst.* **2000**, *C56*, e47−e48. Pelizzi, G. *Inorg. Chim. Acta* **1977**, *24*, L31−L32.
(42) (a) Lockhart, T. P.; Manders, W. F. *Inorg. Chem.* **1986**, *25*, 583−585. (b) Lockhart, T. P.; Manders, W. F.; Schlemper, E. O.; Zuckermann, J. J. *J. Am. Chem. Soc.* **1986**, *108*, 4074−4078.

Table 4. Summary of ^{119}Sn NMR Values and CSA Analysis

compd	δ_{iso}	$\delta_{solution}$	$\delta_{solid} - \delta_{solution}$	δ_{11}	δ_{22}	$\delta 33$	δ	Ω	η	κ
1	−102.4	−114.9	12.5	−53.6	−84.3	−169.0	−66.7	115.4	0.46	0.468
2	−56.5	−41.4	−15.1	85.6	−4.9	−250.2	−193.7	335.8	0.467	0.461
3	−26.3	−32.6	6.3	151.5	151.5	−384.8	−357.5	536.3	0	1
4[a]	−100.5	−115.5	15							
	−108.1		7.4							
4'	−114.8	−115.5	0.7	−59.6	−102.6	−182.0	−67.3	122.4	0.639	0.297
5	−93.1	−46.4	−46.7	29.3	−88.3	−220.4	−127.3	249.7	0.924	0.058
6	−77.4	−48.3	−29.1	165.5	75.4	−471.5	−394.6	636.9	0.228	0.717

[a] Tensor analysis not conducted for **4**.

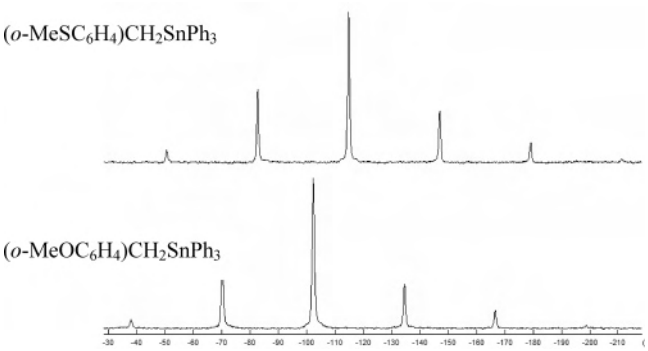

Figure 14. CPMAS ^{119}Sn spectra of **1** and **4′**; spin rate 3000 Hz.

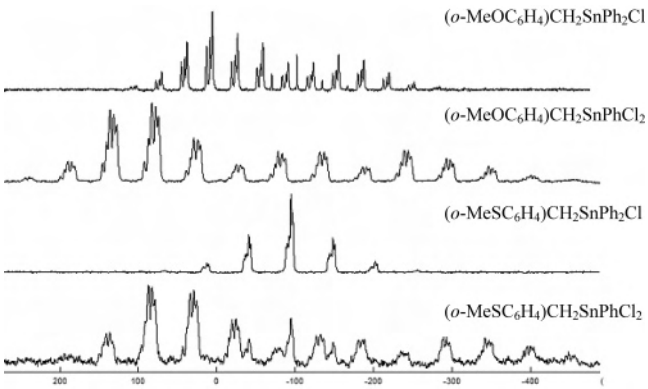

Figure 15. CPMAS ^{119}Sn spectra of **2**, **3**, **5**, and **6**; spin rate 5000 Hz.

tropic chemical shift of −26.3 ppm, a mere 6.3 ppm shift. This surprising result suggests that **3** also retains the O−Sn and Cl−Sn interactions in solution as evidenced by the small $\Delta\delta$. The spectrum of **6** (−77.4 ppm) has a larger upfield shift of 30 ppm compared to its solution state NMR.

Overall, the solid state ^{119}Sn CPMAS NMR chemical shift data of the O-containing compounds **1**−**3** and the S-containing compounds **4**−**6** suggest only minor changes upon going from solution to solid state. A possibly stronger interaction between S and Sn, cf. O and Sn, can be discerned upon changing from solution to solid state.

If the difference between solution and solid-state NMR chemical shift data is too small to map coordination differences, then the distortion of geometry about the tin nuclei can be visualized by the CSA values. Table 4 lists the CSA parameters and their values for compounds **1**−**6**. The principle values δ_{11}, δ_{22}, and δ_{33} are labeled by the suggested IUPAC designation:[43] $\delta_{11} \geq \delta_{22} \geq \delta_{33}$ where $\delta_{iso} = (\delta_{11} + \delta_{22} + \delta_{33})/3$. In addition, values of span ($\Omega = \delta_{11} - \delta_{33}$), skew ($\kappa = 3(\delta_{22} - \delta_{iso})/\Omega$; $-1 \leq \kappa \leq 1$), asymmetry ($\eta = \delta_{yy} - \delta_{xx})/\delta$; $0 \leq \eta \leq 1$), and anisotropy ($\delta = \delta_{zz} - \delta_{iso}$) are included to help understand the environment around tin in these compounds.[31]

Compounds **1** and **4′** have very similar CSA values. The anisotropy (−66.7, −67.3) and the spans (115.4, 122.4) are similar and the lowest of the series illustrate that these two compounds have the most tetrahedral geometry. Although the deviation from tetrahedral geometry is not large, they are distorted by O−Sn or S−Sn interactions, as evidenced by the moderate values of η (0.46, 0.64) and κ (0.47, 0.30).

The diphenyl-chloro compounds **2** and **5** also have anisotropies (−193.7, −127.7) and spans (335.8, 249.7) that are similar, yet as expected, larger than **1** and **4′**. The asymmetry for **5** is close to 1 (0.9), and its skew is very close to 0 (0.06), indicating a very distorted and asymmetric molecule. Indeed, the S−Sn distance of 3.062 Å is enough to fully distort from tetrahedral geometry but not enough to impart the axial symmetry of trigonal bipyramidal geometry. In contrast, the values of η and κ for **2** (0.47, 0.46) illustrate that **2** is not as trigonal bipyramidal as **5** but has a distorted tetrahedral geometry.

Finally, compounds **3** and **6** have the largest anisotropies (−357.5, −394.6) and largest spans (536.3, 636.9) of the series, which indicates that there is a directional dependence of the ^{119}Sn nuclear magnetic field. In other words, the vectors of the CSA components are nonspherical. This is further supported by the η (0, 0.23) and κ (1, 0.72) values of **3** and **6**. For compound **3**, which is pseudo-octahedral, the values of η and κ illustrate axial symmetry, perhaps with δ_{33} parallel to the Cl1−Sn−O or Cl2−Sn−Cl1 axis. Compound **6**, on the other hand, has a low η and high κ value, which supports compound **6** having the most trigonal bipyramidal symmetry of the series imparted by the smallest S−Sn distance (2.99 Å).

Acknowledgment. This research was supported by grants from the Welch Foundation, Houston, TX (Grant No. AH-0546) and the NIH-SCORE program (Grant No. GM-08012). We thank the Kresge Foundation for funds that helped purchase, and help upkeep, our NMR facility. We also thank Professor Guillermo Mendoza Diaz, Universidad de Guanajuato, MX. for many fruitful discussions concerning NMR

(43) (a) *Pure Appl. Chem.* **1972**, *29*, 627 (b) *Pure Appl. Chem.* **1976**, *45*, 217 (c) Harris, R. K.; Kowalewski, J.; De Menezes, S. C. *Pure Appl. Chem.* **1997**, *69*, 2489−2495. (d) Harris, R. K.; Becker, E. D.; De Menezes, S. C.; Goodfellow, R.; Granger, P. *Pure Appl. Chem.* **2001**, *73*, 1795−1818.

spectroscopy. MCL thanks the Universidad Autónoma del Estado de Morelos for a leave of absence.

Supporting Information Available: Listings of crystallographic information files (CIF). This material is available free of charge via the Internet at http://pubs.acs.org.

IC061811S